ICSV13 - Vienna
The Thirteenth International Congress
on Sound and Vibration
Vienna, Austria, July 2-6, 2006

STRUCTURAL AND ACOUSTIC RESPONSE OF BUILDINGS IN THE HIGHER FREQUENCY RANGE DUE TO SURFACE RAIL TRAFFIC

Péter Fiala*[1], Geert Degrande[2], János Granát[1], Fülöp Augusztinovicz[1]

[1]Vibroacoustics and Audio Laboratory, Budapest Univ. of Technology and Economics
Magyar tudósok körútja 2, H-1117, Budapest, Hungary
[2]Structural Mechanics, K.U.Leuven
Kasteelpark Arenberg 40, B-3001 Leuven
fiala@hit.bme.hu

Abstract

This paper deals with the numerical computation of the structural and acoustic response of a building to an incoming wave field generated by high-speed railway traffic at grade. The source model consist of the model of a moving vehicle on a longitudinally invariant domain coupled to a boundary element model of the underlying ground. The receiver model is based on a substructuring formulation and consists of a boundary element model of the soil and a finite element model of the structure. The acoustic response of the building's rooms is computed by means of a standard boundary element formulation. The paper investigates the structural and acoustic response of a multi-story portal frame office building.

INTRODUCTION

Traffic induced vibrations in dense urban environments can cause undesired effects in surrounding buildings, as well as annoyance to the inhabitants. Therefore, the prediction of traffic induced vibrations and re-radiated sound is of high importance. The present paper discusses numerical methods used to model structural vibrations and re-radiated noise induced by railway traffic at grade. A full 3D approach is used, and the whole vibration path is discussed starting from vibration generation by a moving high-speed train, and ending with the re-radiated noise in an enclosure of a building. As not only structural vibrations but noise radiation is investigated, the upper frequency limit of computations is 200 Hz.

METHODOLOGY

The incident wave field

A 2.5D frequency-wavenumber domain method is used to determine the free-field ground vibrations generated by the passage of a train on an uneven track [3]. The train model consists of a number of concentrated masses, moving along the track, and representing the vehicle's axles. The invariant track model consists of two Euler beams representing the rails, distributed mass modelling the sleepers, and a distributed spring-damper system representing the rail pads and the ballast [2].

The soil is modelled as a layered half-space. A 2.5D frequency-wavenumber domain boundary element method (BEM) [1] using the Green's functions of a layered half-space is used to compute the soil's impedance. This impedance is coupled to that of the track system in order to determine the dynamic loads acting on the soil-track interface. The Green's funtions of the layered half-space are used to determine the free-field response due to the moving source.

The structural response and Soil-structure interaction

The finite structure is modelled in the frequency domain by a 3D structural finite element method (FEM). A Craig-Bampton [4] modal decomposition method is used. The total displacement of the structure is computed as a superposition of the quasi-static transmission of foundation modes and the modes of the superstructure clamped at the foundation.

In order to fully account for soil-structure interaction (SSI), the impedance of the soil and the forces acting on the soil-structure interface are computed by means of a 3D BEM [5] for the layered soil domain.

Acoustic response

An acoustic 3D BEM is used to compute the re-radiated sound field in an enclosure of the building. No coupling between the structural and acoustic response is accounted for, so the structural response is used as a velocity constraint in the BE model. The structural and acoustic surface velocities are coupled through an impedance value representing the absorption of the walls. Below 200 Hz, the wall's impedance can be estimated from the absorption coefficient assuming plane wave behaviour and perpendicular incidence.

NUMERICAL EXAMPLE

The incoming wave field

A Thalys high-speed train [3] travelling with a velocity of $v = 80$ m/s on an uneven rail is modelled. The 200 m long train consists of two locomotives and eight carriages, having a total number of 26 axles distributed over 13 bogies. Each axle is modelled by a concentrated mass of 2027 kg.

Table 1: *Dimensions of the track system*

Rail gauge	1.435 m	Ballast mass	1750 kg/m
Rail bending stiffness	6.489×10^6 Nm^2	Ballast stiffness	125.8×10^6 N/m^2
Rail mass	60.8375 kg/m	Ballast damping	41.3×10^3 Ns/m^2
Railpad stiffness	235.6×10^6 N/m^2	Sleeper dimensions	$2.5 \times 0.24 \times 0.21$ m
Railpad damping	25.1×10^3 Ns/m^2	Sleeper density	2500 kg/m^3

The track is modelled as a conventional ballasted track consisting of a pair of rails, elastic rail pads, concrete sleepers and a ballast layer. The dimensions and material properties of the track elements are given in Table 1. The smeared mass, damping and stiffness values are given for a unit length along the track. The soil is considered to be a homogeneous elastic halfspace with a shear wave velocity $C_S = 300$ m/s, a mass density $\rho = 1750$ kg/m^3, Poisson's ratio $\nu = 1/3$, and a hysteretic material damping coefficient $\beta = 0.025$. The source of dynamic excitation is the rail unevenness that is characterized by its power spectral density in the wavenumber domain.

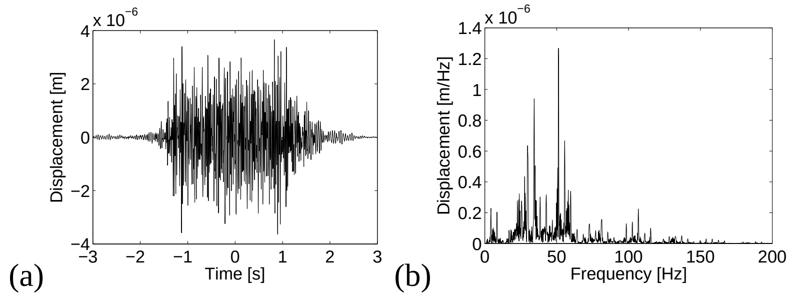

Figure 1: *(a) time history and (b) frequency content of free field vertical ground displacements*

The frequency content and time history of the vertical component of the incident displacement wave field is plotted in Figure 1. The dominating part of the frequency content is between 20 Hz and 80 Hz, but vibrations above 125 Hz are also present. The time history extends from -2 s until 2 s. The equidistant peaks correspond to the 13 bogies of the train.

The office building model

The position of the railway track and the building, as well as the FE mesh of the two-story portal frame building model are plotted in Figure 2. The building's dimensions are 20 m $\times$ 12 m $\times$ 7 m. The superstructure is supported by a raft foundation. Only the basic structure consisting of three horizontal slabs (including the foundation), the portal frame structure and a central core, as well as the in-fill walls of a single room besides the core are taken into account in the discretized model. The element size is chosen to 0.25 m, which is fine enough for computations up to 200 Hz. The model has

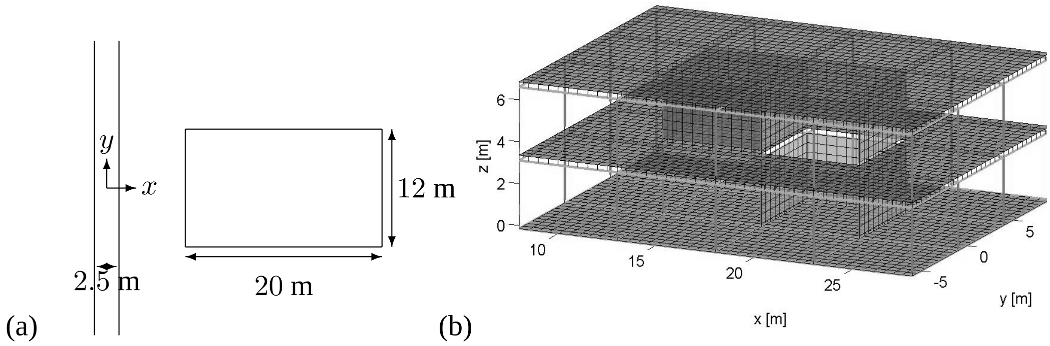

Figure 2: *(a) Ground plan of the site and (b) FE mesh of the office building*

91218 degrees of freedom. In order to have a sufficient modal base, all the modes (313 foundation and 818 superstructure modes) up to 400 Hz have been determined and are used in the Craig-Bampton modal synthesis.

The impedance of the soil

For the computation of the soil impedance the same foundation mesh as presented in figure 2b has been used. Due to the time demand of computations, the impedance has been computed only up to 100 Hz. Figure 3 introduces the soil impedance projected on the vertical rigid body displacement mode of the foundation. The impedance $S(\omega)$ is presented by dimensionless spring $k(\omega)$ and damping $c(\omega)$ coefficients, defined as $S_(\omega) = K_0(k(\omega) + ia_0c(\omega))$, where $a_0 = \omega R/c_S$ denotes dimensionless frequency, R is equivalent radius of the foundation, and K_0 denotes the static impedance of a rigid massless foundation of radius R on an elastic halfspace. The functions show slowly decaying spring and constant damping coefficients, meaning that increasing frequency the damping dominates the soil's impedance.

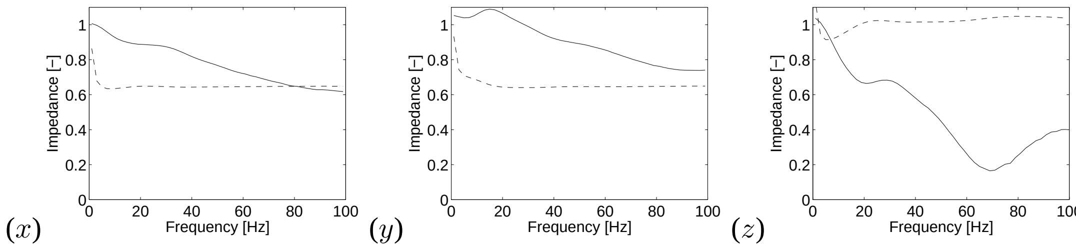

Figure 3: *Spring (solid line) and damping (dashed line) coefficients of the soil impedance projected on the rigid body displacement modes of the foundation.*

Structural response

In the following, the structural response of the office building is presented. Three cases are considered. In case 1, the foundation of the building is considered to be rigid, and no SSI is taken into account. The incident wave field is projected on the six rigid body modes of the structure, and the resulting displacement is considered as a displacement constraint of the structure. In case 2, a flexible foundation is considered without SSI taken into account: the incoming wave field is considered as a displacement excitation of the structure. In case 3, the foundation is considered to be flexible, and SSI is accounted for.

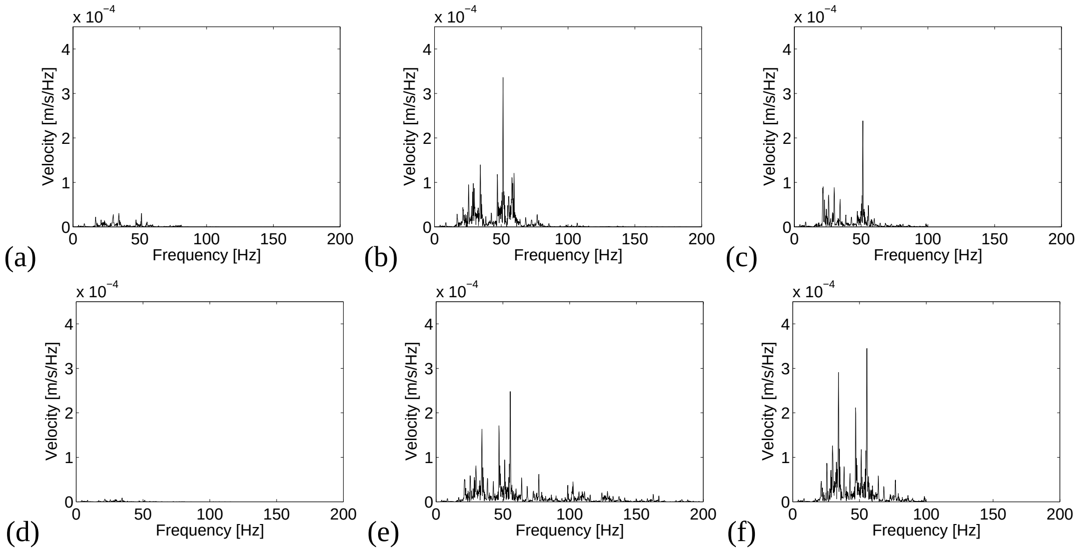

Figure 4: *Vertical structural velocity in point P2 (first row) and point P1 (second row) for case 1 (first column), case 2 (second column) and case 3 (third column).*

Figure 4 displays the structural displacements in two points, P1 and P2 of the building for all the three cases. The point P1 is located on the ground level, P2 is located on the floor of the room, both at coordinates $x = 15.5$ m, $y = 0$ m. Figure 4e – corresponding to flexible foundation without SSI – displayes the incident free field velocity in P1. The wave field has important components between 20 Hz and 150 Hz. Comparing Figures 4d and 4e, it can be stated that assuming a rigid body motion of the foundation results in the total suppression of the incident wave field. Furthermore, it can be seen that the vibrations above 100 Hz are not transmitted up to the first floor, due to structural damping in the building. SSI results in a suppression of high-frequency incident velocity components, as well as a slight attenuation of the vibration levels on the room's floor.

Acoustic response in the room

Figure 5 displays the deformed FE mesh of the room (a part of the total office model of dimensions 5 m $\times$ 4 m $\times$ 3.1 m) for a mode of the superstructure, as well as the acoustic BE mesh, colored using the same displacements projected on the internal normal vector.

The sound velocity is equal to $C = 343$ m/s, and the density of the air is $\rho = 1.225$ kg/m^3. Three different absorption coefficients are considered: $\alpha_1 = 0$ describes

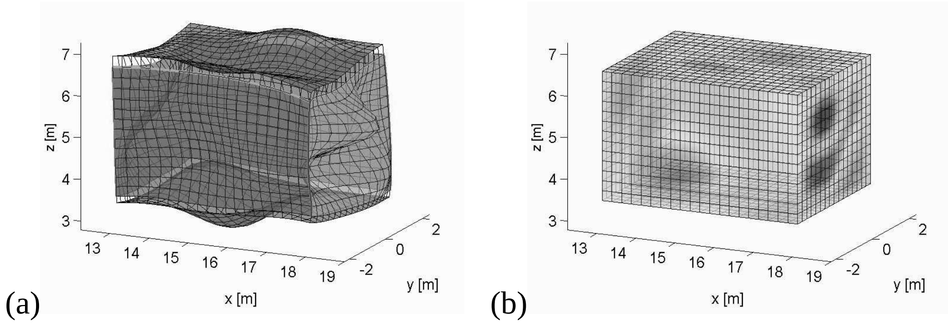

Figure 5: *(a) FE and (b) BE meshes of the room*

an extreme case of no absorption, $\alpha_2 = 0.03$ stands for strongly reflecting room with uncarpeted concrete floor, $\alpha_3 = 0.15$ is typical for an unfurnished carpeted room. Using the Sabine formula giving an approximation of the reverberation time t_{rev} as a function of the room's volume, the surface area and the average absorption coefficient, $t_{\text{rev}_1} = \infty$, $t_{\text{rev}_2} = 3.45$ s and $t_{\text{rev}_3} = 0.69$ s are obtained.

Figure 6 shows the acoustic transfer between the displacement of a room node at $\{8.50\text{ m}, 10\text{ m}, 5.17\text{ m}\}$ and an internal point P3 at $\{8.46\text{ m}, 6.17\text{ m}, 5.83\text{ m}\}$. The frequencies of the room's horizontal and vertical resonances (where the acoustic wavelength is equal to a multiple of the room's wall lengths) are marked by dotted lines in Figure 6a. The effect of the walls' absorption is clearly visible in the figures. The sharp peaks at the room's resonances disappear for high absorption. The time histories show that the higher absorption results in smaller magnitude and reverberation time of the impulse responses.

Figure 7 plots the time history and one-third octave band spectra of the sound pressure in point P3 for the absorption coefficients α_1 and α_2, and all the three cases regarding SSI. As for the case of the structural vibrations, very low sound pressure levels are observed for the case of the rigid surface foundation. The flexible foundation without SSI results in the highest sound pressure levels. The dominating one-third octave bands are those containing the room resonances at 34 Hz (first horizontal resonance in the x direction), 55 Hz (first vertical resonance) and 68 Hz (second horizontal resonance in the x direction). A difference of 5 dB between the two wall absorptions can be observed above the first acoustic resonance. Comparing cases 2 and 3, it can be seen that dynamic SSI results in an attenuation of 10 dB above 50 Hz. Amplification can also be observed at the frequency band of 31 Hz containing the first eigenfrequency of the room, but only for the low absorption coefficient.

The time history diagrams clearly show that the lower absorption causes not only higher sound pressure levels, but as expected, longer reverberation times. The total pass-by can be divided into 13 segments corresponding to the 13 bogies of the HST.

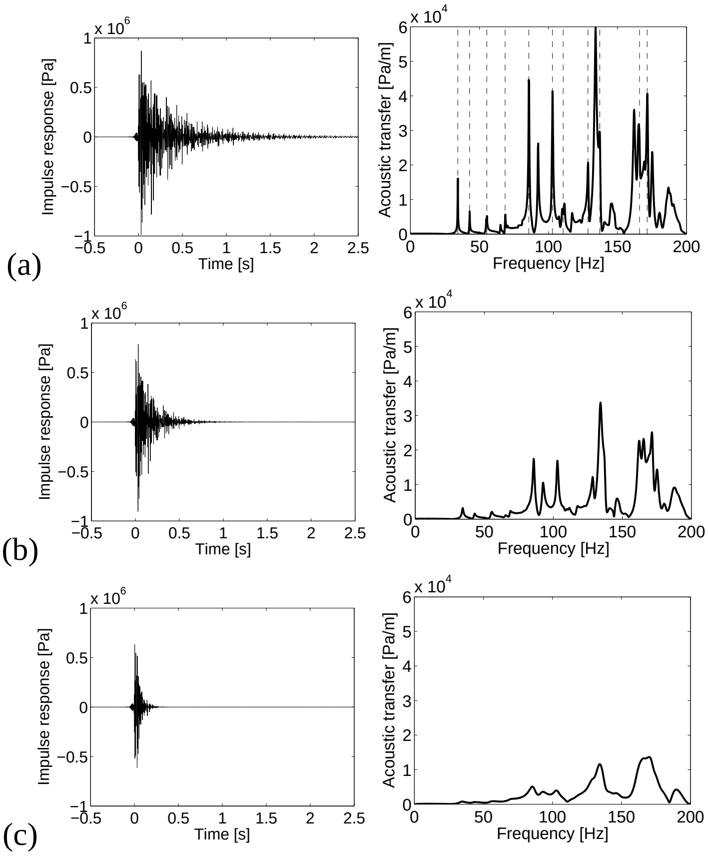

Figure 6: *Impulse response (left hand side) and transfer function (right hand side) between the displacement at a node of the room surface and the pressure in the point P3 for an absorption coefficient (a)* $\alpha = 0$*, (b)* $\alpha = 0.03$ *and (c)* $\alpha = 0.15$

CONCLUSIONS

A 3D numerical model has been presented that is capable to predict surface traffic induced vibrations and re-radiated sound in builings, accounting for a moving vibration source, vibration propagation in a layered ground, dynamic soil-structure interaction and sound radiation into acoustic enclosures.

A numerical example has been used to demonstrate the use of the methods. The structural and acoustic response of a two-story portal frame office building has been calculated up to the frequency limit of 200 Hz. It has been shown that the dominant frequencies of the traffic induced acoustic response are basically determined by the first acoustic resonances of the room. The effect of wall absorption on the pressure response has been investigated, and above the first acoustic resonance, a difference of 5 dB has been found between typical wall absorptions for concrete and carpeted walls. Regarding the effect of dynamic SSI on the internal pressure levels, the radiation damping of the soil has been found as an important factor in the dominant frequency range.

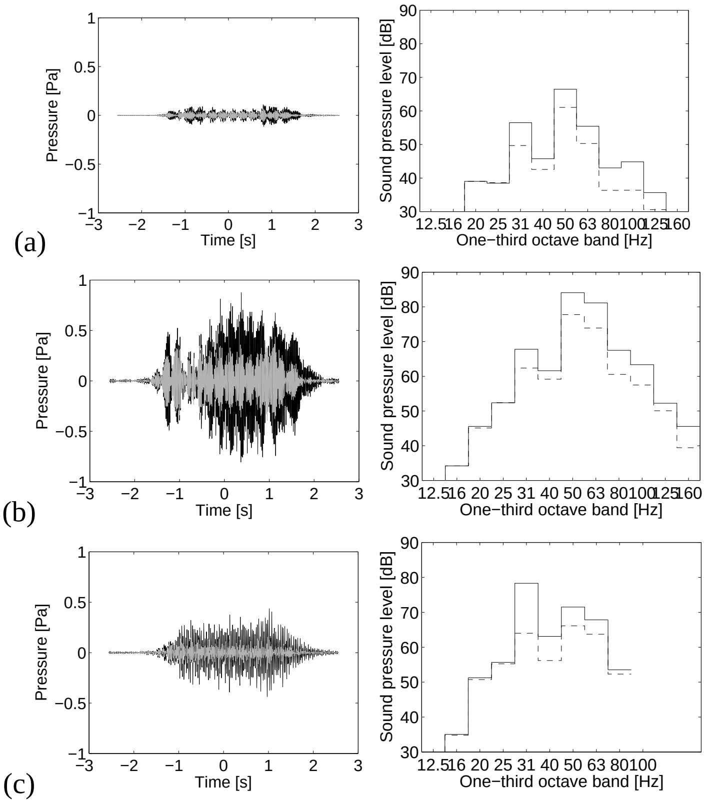

Figure 7: *Pressure time history (left hand side) and one-third octave band levelel (right hand side) in the point P3 during the the passage of a HST for (a) case 1, (b) case 2 and (c) case 3.*

ACKNOWLEDGEMENTS

The results presented in this paper have been obtained within a bilateral cooperation founded by the Flemish Community and the Hungarian Scholarship Board. Their financial support is gratefully acknowledged.

REFERENCES

[1] G. Lombaert, G. Degrande, D. Clouteau. Numerical modelling of free field traffic induced vibrations. *Soil Dynamics and Earthquake Engineering*, **19(7)**:473–488, 2000

[2] P. Fiala, J. Granát, F. Augusztinovicz. *Modelling of ground vibrations in the vicinity of a tangent railway track*. Forum Acusticum 2005, Budapest, 2005

[3] G. Lombaert, G. Degrande, J. Kogut, S. François. The experimental validation of a numerical model for the prediction of railway induced vibrations. *Journal of Sound and Vibration*, In press, 2006

[4] R.J. Craig and M. Bampton. Coupling of substructures for dynamic analyses. *AIAA Journal*, **6(7)**:1313–1318, 1968

[5] D. Aubry, D. Clouteau. A subdomain approach to dynamic soil-structure interaction. In V.Davidovici and R.W.Clough, editors, *Recent advances in Earthquake Engineering and Structural Dynamics*, pp251-272. Ouest Editions/AFPS, Nantes, 1992

[6] W.C. Sabine. *Collected Papers on Acoustics*. Peninsula Publishing, Los Altos, 1993.